J Mol Model (2012) 18:2699–2708
DOI 10.1007/s00894-011-1246-6

ORIGINAL PAPER

Methane storage in homogeneous armchair open-ended single-walled boron nitride nanotube triangular arrays: a grand canonical Monte Carlo simulation study

Sayyed Jalil Mahdizadeh · Sayyed Faramarz Tayyari

Received: 23 June 2011 / Accepted: 14 September 2011 / Published online: 20 November 2011

Abstract The physisorption of methane in homogeneous armchair open-ended SWBNNT triangular arrays was evaluated using grand canonical ensemble Monte Carlo simulation for tubes 11.08, 13.85, 16.62, and 19.41 Å [(8,8), (10,10), (12,12), and (14,14), respectively] in diameter, at temperatures of 273, 298, 323, and 373 K, and at fugacities of 0.5–9.0 Mpa. The intermolecular forces were modeled using the Lennard–Jones potential model. The absolute, excess, and delivery adsorption isotherms of methane were calculated for the various boron nitride nanotube arrays. The specific surface areas and the isosteric heats of adsorption, Q_{st}, were also studied, different isotherm models were fitted to the simulated adsorption data, and the model parameters were correlated. According to the results, it is possible to reach 108% and 140% of the US Department of Energy's target for CH_4 storage (180 v/v at 298 K and 35 bar) using the SWBNNT array with nanotubes 16.62 and 19.41 Å in diameter, respectively, as adsorbent. The results show that for a van der Waals gap of 3.4 Å, there is no interstitial adsorption except for arrays containing nanotubes with diameters of >15.8 Å. Multilayer adsorption starts to occur in arrays containing nanotubes with diameters of >16.62 Å, and the minimum pressure required for multilayer adsorption is 1.0 MPa. A brief comparison of the methane adsorption capacities of single-walled carbon and boron nitride nanotube arrays was also performed.

S. J. Mahdizadeh (✉)
Department of Chemistry, Ferdowsi University of Mashhad,
Mashhad 91775-1436, Iran
e-mail: sj.mahdizadeh@stu-mail.um.ac.ir

S. F. Tayyari
Chemistry Department, Islamic Azad University,
Shahrood Branch,
Shahrood, Iran

Keywords GCMC simulation · Methane storage · SWBNNT · Adsorbed natural gas · 12–6 Lennard–Jones potential model

Introduction

Boron nitride nanotubes (BNNTs) can be considered rolled-up hexagonal BN sheets or carbon nanotubes (CNTs) in which the C atoms have been replaced with alternating B and N atoms. In 1981, Ishii et al. reported the discovery of one-dimensional boron nitride nanostructures that have a bamboo-like structure. These were named BN whiskers [1]. However, nanoscale BN with a perfect tubular structure was first predicted in 1994 [2, 3], before it was actually synthesized by arc discharge in 1995 [4]. Various methods, such as laser ablation [5], chemical vapor deposition (CVD) [6], ball-milling [7], and a substitution reaction [8], have been invented and used to synthesize BNNTs.

These materials, due to their unique physicochemical features, have been considered for various applications, especially theoretical and experimental adsorption studies—for example, the adsorption of H_2 [9–20], atomic hydrogen [21], O_2 [9, 22], N_2 [9], H_2O [9, 23], Li [24, 25], Be, C, F [25], Ni [26, 27], Sc, Ti, V, Cr, Mn, Fe, Co, Cu, Zn, Pd, and Pt [27], and nucleobases [28]—but there is no comprehensive paper on methane adsorption in BNNTs in the literature.

As human society has developed and progressed technologically, the consumption of fossil fuels (coal, petroleum, and others) has increased drastically. New and effective alternative energy sources are thus urgently required. On the other hand, in order to control emissions, clean fuels are needed for vehicles. Thus, various environmentally friendly fuels and related

technologies are being developed to replace fossil fuels. For example, numerous studies have been carried out on the application of natural gas as a clean energy fuel [29–32]. Compared with petrol, natural gas is a much cleaner fuel. There are a variety of methods for storing natural gas, including compression, liquefaction, dissolution, clathration, and adsorption. Compression is the fuel storage technique currently used for natural gas vehicles. In order to achieve a substantial capacity, very high storage pressures are used, and are likely to increase to ~250 bars. Therefore, the tanks are heavy, expensive, and unsafe. Storing natural gas through adsorption involves using the micropores in adsorbent materials. Because adsorption potentials are strongly enhanced in micropores, the density of the adsorbed phase can be higher than that of liquid natural gas. The main advantage of adsorbed natural gas over compressed natural gas is that it reduces the storage pressure, thereby reducing the cost and increasing safety. SWBNNTs are one of the best candidates for the adsorbing material in adsorbed natural gas procedures due to their large specific surface area and abundance of sites at which gases can react.

Methane is the major component of natural gas; therefore, in order to achieve the optimum conditions for adsorbed natural gas processes, the adsorption behavior of methane in various situations must be explored. With this in mind, the purpose of this study was to theoretically evaluate methane physisorption in SWBNNT triangular arrays containing nanotubes of various diameters, and at various temperatures and pressures. To attain these goals, we used grand canonical Monte Carlo (GCMC) simulation of nanotubes with diameters of 11.08, 13.85, 16.62, and 19.41 Å at temperatures of 273, 298, 323, and 373 K and at fugacities of 0.5–9.0 Mpa.

GCMC simulation details

Methane adsorption in SWBNNT arrays was investigated using the MUSIC simulation package from Gupta and coworkers [33], with CH_4–CH_4, CH_4–N, and CH_4–B interactions modeled by the 12–6 Lennard–Jones potential model, which is expressed as follows:

$$\Phi_{ij}(r) = 4\varepsilon_{ij}\left[\left(\frac{\sigma_{ij}}{r}\right)^{12} - \left(\frac{\sigma_{ij}}{r}\right)^{6}\right], \quad (1)$$

where r denotes the intersite distance, and ε and σ denote the LJ energy parameter and the well-depth parameter, respectively. The Lorentz–Berthelot mixing rules were used to calculate the mixed Lennard–Jones parameters [34]. Methane was represented by the united-atom model, which describes a single interaction site. The LJ potential parameters are listed in Table 1. No electrostatic interactions were considered between methane molecules or between methane and BNNTs.

Table 1 LJ parameters and their sources

Center	σ (Å)	ε/k_B (K)	Reference
CH_4	3.73	148	[35]
Nitrogen	3.36	72.89	[20]
Boron	3.45	47.76	[20]

The nanotube arrays consisted of boron nitride nanotubes in the armchair configuration with varying diameters. The N–B distance was set to 1.45 Å, based on crystallographical data [36]. The single tubes of the first array had diameters of 11.08 Å and were arranged in a triangular array with a distance of 3.4 Å between two adjacent tubes (8,8) [37, 38]. Furthermore, three arrays with the same VDW gap but different pore diameters of 13.85 Å (10,10), 16.62 Å (12,12), and 19.41 Å (14,14) were included in this study. A typical unit cell is illustrated in Fig. 1.

The GCMC simulations were carried out at various temperatures and pressures in order to calculate adsorption isotherms. Deformations can occur for larger nanotubes, but note that the nanotubes investigated in this study were not very large ($11.08 \leq D \leq 19.41$ Å); in addition, framework flexibility has only a tiny effect on adsorption isotherms [39]. Therefore, we simulated all nanotubes as "perfect" SWBNNTs, and all of the nanotubes were modeled as a rigid framework. The length of each nanotube was set to 23.7 Å, and periodic boundary conditions were applied at all interfaces during displacement. In the grand canonical ensemble, the number of particles can fluctuate, whereas

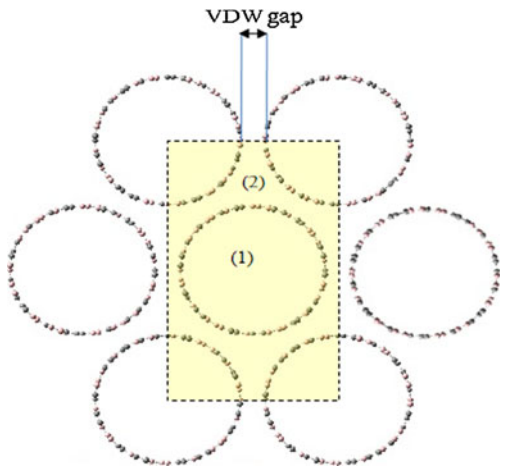

Fig. 1 Different adsorption sites and the unit cell (*shaded area*) in a homogeneous triangular array of SWBNNTs: (*1*) intratubular, (*2*) interstitial channel

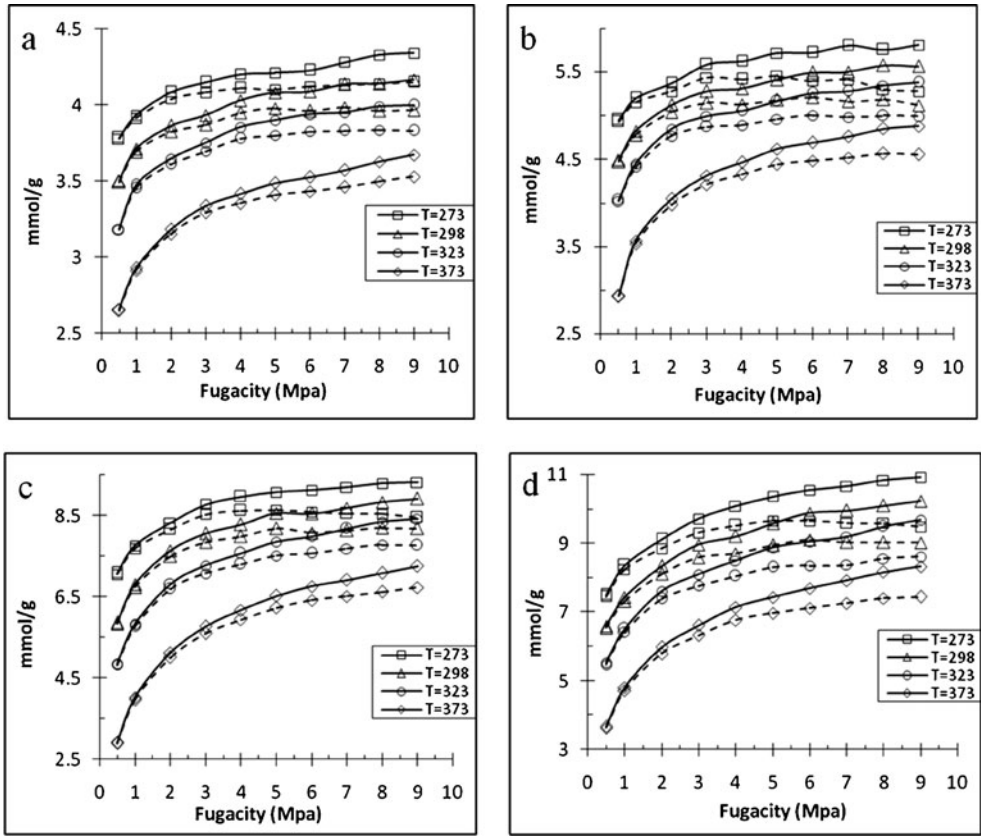

Fig. 2 Adsorption isotherms of methane in various SWBNNT triangular arrays: D=11.08 Å (**a**), D=13.85 Å (**b**), D=16.62 Å (**c**), D=19.41 Å (**d**). *Solid lines* are absolute adsorption and *dashed lines* are excess adsorption

the chemical potentials, the temperature and the volume are kept constant. For details about the GCMC method, see [40]. The GCMC simulations were carried out with 5×10^6 equilibration steps and another 5×10^6 production steps to collect the data at each value of the imposed pressure. Interactions at separations of >9.5 Å, which correspond to 2.5 times the σ parameter for methane, were neglected. Either the bulk chemical potentials or the bulk fugacities must be specified for the molecule exchange acceptance rules [41]. The fugacities were calculated using the Peng–Robinson equation of state, with parameters taken from [42].

The excess number of molecules, n^{ex}, is related to the absolute number of molecules, n^{abs}, by

$$n^{ex} = n^{abs} - \frac{PV^g}{ZRT}, \quad (2)$$

where V^g is the pore volume of the adsorbent, and Z is the compressibility factor in the bulk gas phase at equilibrium temperature and pressure, calculated with the Peng–Robinson equation of state. P, T, and R are the pressure, temperature, and the universal gas constant (8.3145 J mol^{-1} K^{-1}), respectively.

To calculate V^g, we used the method described in [43].

Results and discussion

Adsorption uptake isotherms of methane in various SWBNNT triangular arrays are presented in Fig. 2. In practical applications of porous material for gas storage, the delivery uptake—the difference between the total amount at pressure p and that at 5 bar—is an important quantity [44], so delivery uptake isotherms were calculated and are presented in Fig. 3. Upon comparing the Figs. 2d and 4, it is obvious that the SWBNNTs are a far more preferable storage material than single-walled carbon nanotubes (SWCNTs) for methane storage processes. In order to clarify why this is the case, Fig. 5 shows the methane storage capacity ratios of SWBNNT and SWCNT with nanotubes of almost the same diameter (D=19.00 Å for SWCNT and D=19.41 Å for SWBNNT) at different temperatures and pressures. As seen from Fig. 5, the methane loading ratio at low pressures is much greater than that at high pressures, and this ratio also increases as the temperature increases. For example, at 0.5 Mpa, this ratio is 172, 209, 248, and 328% at temperatures of 273, 298, 323, and 373 K, respectively. This conclusion is in accord with those reported earlier for hydrogen adsorption [10, 11, 20].

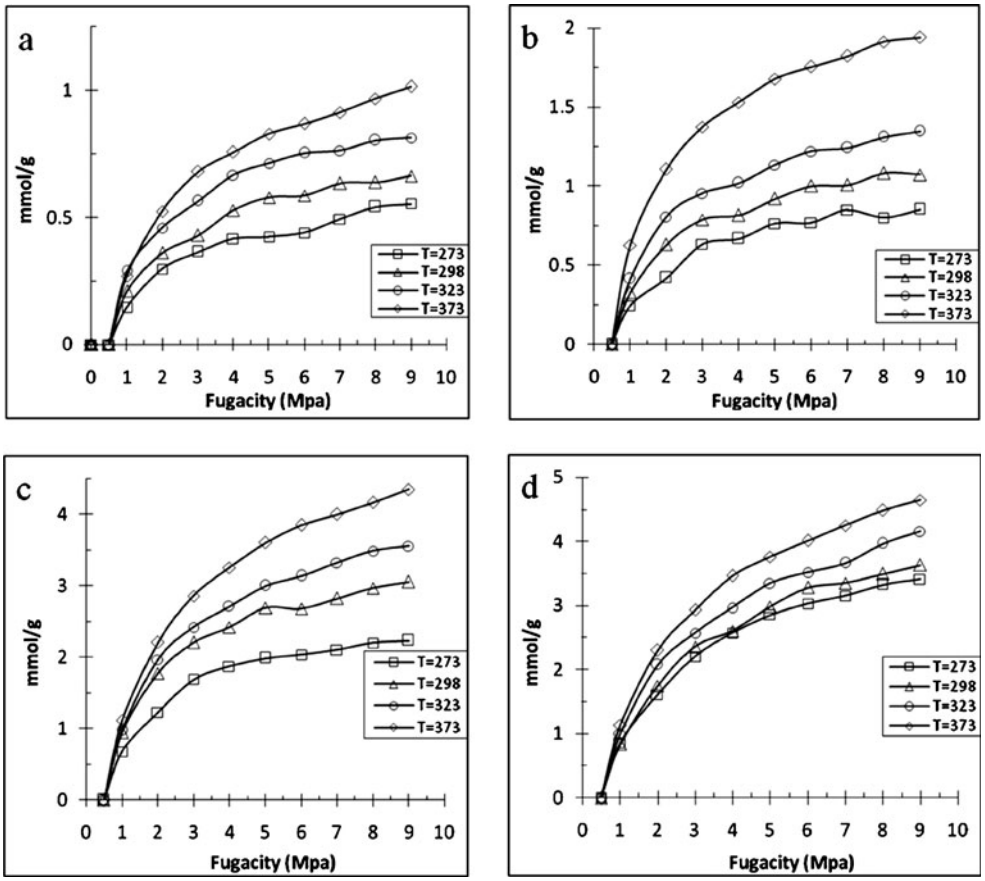

Fig. 3 Delivery uptake isotherms of methane in various SWBNNT triangular arrays: D=11.08 Å (**a**), D=13.85 Å (**b**), D=16.62 Å (**c**), D=19.41 Å (**d**)

Figure 6 shows the total methane uptake (v/v) isotherms for arrays with D=16.62 (12,12) and D=19.41 Å (14,14) at a temperature of 298 K. As can be seen in Fig. 6, it is possible to achieve 108% and 140% of the US Department of Energy's target for CH_4 storage (180 v/v at 298 K and 35 bar) using the SWBNNT array with nanotube diameters of 16.62 and 19.41 Å, respectively.

The results show that for a van der Waals (VDW) gap of 3.4 Å, no interstitial adsorption is observed except for arrays containing nanotubes with diameters of >15.8 Å. This conclusion is in agreement with results reported by Mahdizadeh and Tayyari [43] and Talapatra and Migone [45] for methane adsorption in SWCNT arrays.

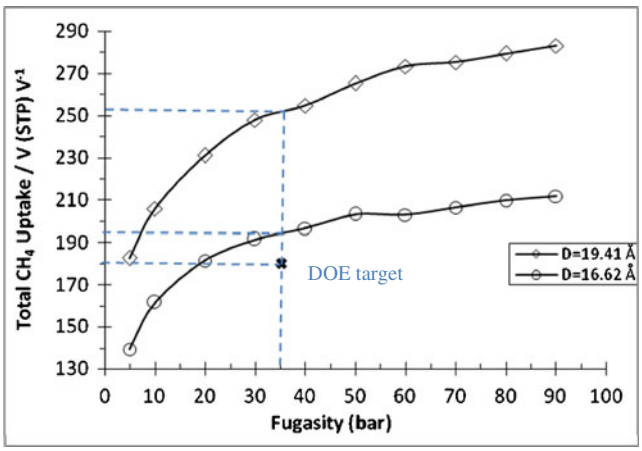

Fig. 4 Total CH_4 uptake isotherms for arrays with nanotube diameters of 16.62 and 19.41 Å at a temperature of 298 K

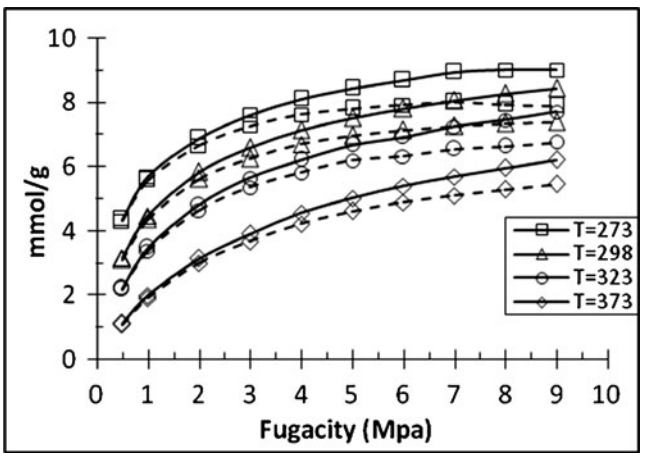

Fig. 5 Adsorption isotherms of methane in SWCNT triangular arrays with D=19.00 Å. *Solid lines* are absolute adsorption and *dashed lines* are excess adsorption [43]

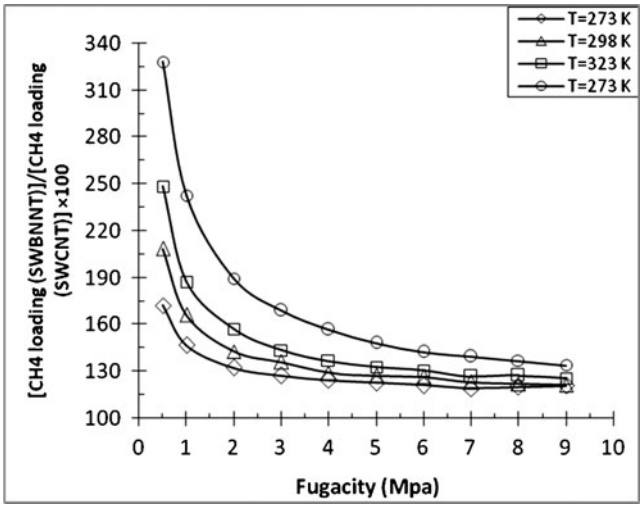

Fig. 6 Methane storage capacity ratios for SWBNNT and SWCNT with almost the same nanotube diameter (D=19.00 Å for SWCNT and D=19.41 Å for SWBNNT) at different temperatures and pressures

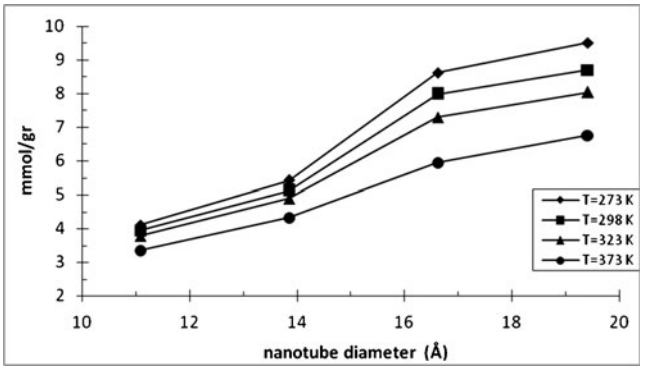

Fig. 8 Total amount adsorbed as a function of nanotube diameter at different temperatures and constant pressure (P=4.0 MPa)

Figure 7 shows some snapshots of methane molecules in different nanotube arrays at P=4.0 Mpa and T =273 K. The interstitial adsorption occurs only for nanotube arrays with D=16.62 and 19.41 Å, as can be seen in Fig. 7c and d. Figure 8 compares the amount adsorbed as a function of nanotube diameter at the studied temperatures and with P=4.0 Mpa.

In order to study the effect of pressure on multi-layer adsorption and to compare interstitial and intratubular adsorption, we took some snapshots of the simulation cell for methane adsorption in (12,12) and (14,14) SWBNNT arrays at different pressures and a constant temperature of 298 K (Figs. 9 and 10). According to the simulation results, multi-layer adsorption starts to occur in arrays with nanotube diameters of >16.62 Å, and the minimum pressure required for multi-layer adsorption is 1.0 MPa.

It is more interesting to compare interstitial and intratubular adsorption for two arrays that exhibit interstitial adsorption [(12,12) and (14,14)]. As seen from Fig. 9, interstitial adsorption in the (12,12) SWBNNT array starts at the lowest pressure investigated (5 bar), while multi-layer adsorption starts at P=10 bar and increases as the pressure increases. Also, the contribution of interstitial adsorption to the total amount adsorbed increases as the pressure increases. On the other hand, for the (14,14) SWBNNT array, while interstitial adsorption increases slightly as pressure increases, the contribution of interstitial adsorption to the total amount adsorbed shows the opposite behavior. The results are shown in Figs. 11 and 12. These figures indicate that at low pressures, about 15 and 26% of the total adsorption occurs at the interstitial sites for (12,12) and (14,14) SWBNNT arrays, respectively.

Different isotherm models (the Langmuir, Freunlich, and Sips models) were fitted to the simulated adsorption data at T= 298 and 373 K, and the model parameters were correlated. The results are presented in Table 2. The proposed isotherm models are described in the "Appendix." Among the models, the Sips isotherm model, on average, shows the best agreement with the simulated data in all cases. The Sips adsorption isotherm model is the method that is frequently applied in work on gas adsorption. The advantages of this

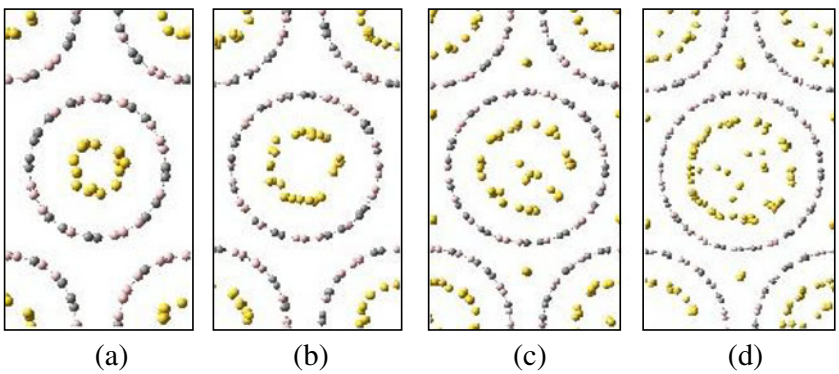

Fig. 7 Snapshots of methane molecules in nanotube arrays with different nanotube diameters and a VDW gap of 3.4 Å at P=4.0 MP and T=273 K. D=11.08 Å (**a**), D=13.85 Å (**b**), D=16.62 Å (**c**), D=19.41 Å (**d**)

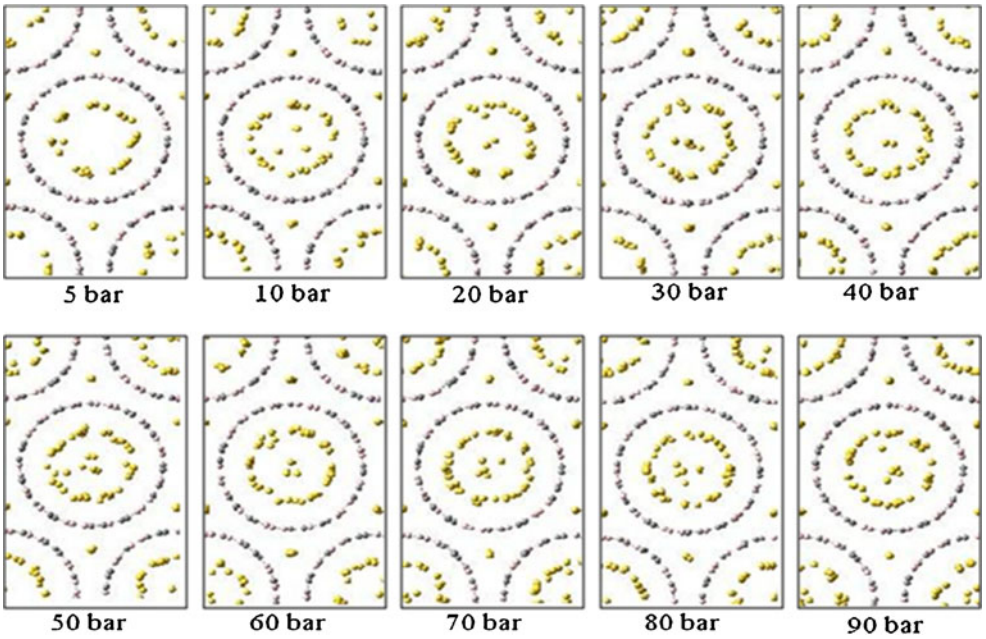

Fig. 9 Snapshots of methane molecules in a SWBNNT array with D=16.62 Å at different pressures

model are its ability to fit simulation data, its mathematical simplicity, and the fact that it can be extended in a straightforward manner to multi-component adsorption. This model also allows multi-layer adsorption to be studied, such as the methane adsorption in (12,12) and (14,14) BNNT arrays. For these reasons, the Sips model is predominantly used in the modeling and design of adsorbents.

The isosteric heat of adsorption, Q_{st}, can be obtained by the Clausius–Clapeyron equation:

$$Q_{st} = -R\left[\frac{\partial \ln P}{\partial\left(\frac{1}{T}\right)}\right]. \tag{3}$$

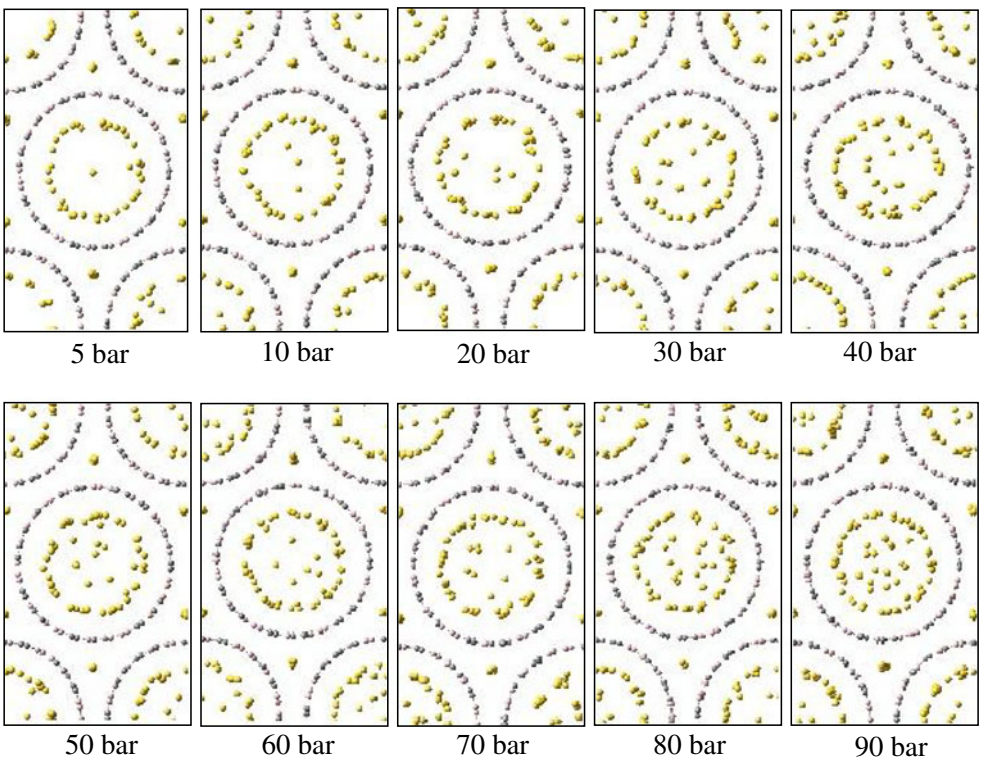

Fig. 10 Snapshots of methane molecules in a SWBNNT array with D=19.41 Å at different pressures

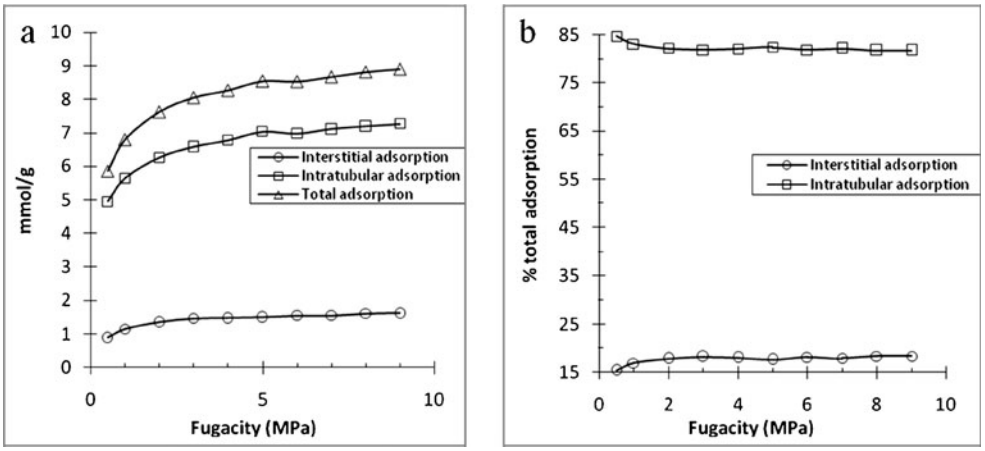

Fig. 11 Interstitial, intertubular, and total adsorption isotherms of methane in a (12,12) SWBNNT array at T=298 K (**a**); contributions of interstitial and intertubular adsorption to the total adsorption (**b**)

Here, P is the pressure, T is the temperature, R is the gas constant, and Q_{st} is the isosteric heat of adsorption. The logarithmic form of the equilibrium pressure was plotted against the reciprocal temperature at constant coverage. The slopes of these lines (which represent the isosteric heat of adsorption) were calculated. Figure 13 shows these plots for five different adsorbed amounts. The results indicate that the isosteric heat of adsorption decreases as nanotube diameter increases (Fig. 14). This is consistent with the observation that smaller nanotubes have greater curvature, so the boron and nitrogen hybridizations, as determined by the N–B–N and B–N–B bond angles, are more consistent with sp^3, leading to a stronger interaction with CH_4. Peralta-Inga et al. [46] reported that the magnitudes of both the positive and negative surface potentials associated with the boron nitride nanotubes tend to be larger where the curvature is greater. This result was also observed in the interactions of carbon nanotubes with methane molecules [43].

We also calculated the specific surface areas of different arrays using the Brunauer–Emmett–Teller (BET) and Langmuir models. The results are presented in Table 3. It is obvious that the BET model yields much more accurate predictions for the specific surface area than the Langmuir model considering the experimentally derived values were 200–700 m^2/g [18, 47].

Conclusions

We used GCMC simulation in order to investigate the influence of temperature, pressure, and nanotube diameter on methane adsorption by homogeneous armchair open-ended SWBNNT triangular arrays. To do this, we calculated the absolute and excess adsorption isotherms of methane in various boron nitride nanotube arrays. The specific surface areas and the isosteric heats of adsorption, Q_{st}, were also studied. Different isotherm models were fitted to the simulated adsorption data, and the model parameters were correlated. According to the results, it is possible to achieve 108% and 140% of the US Department of Energy's target

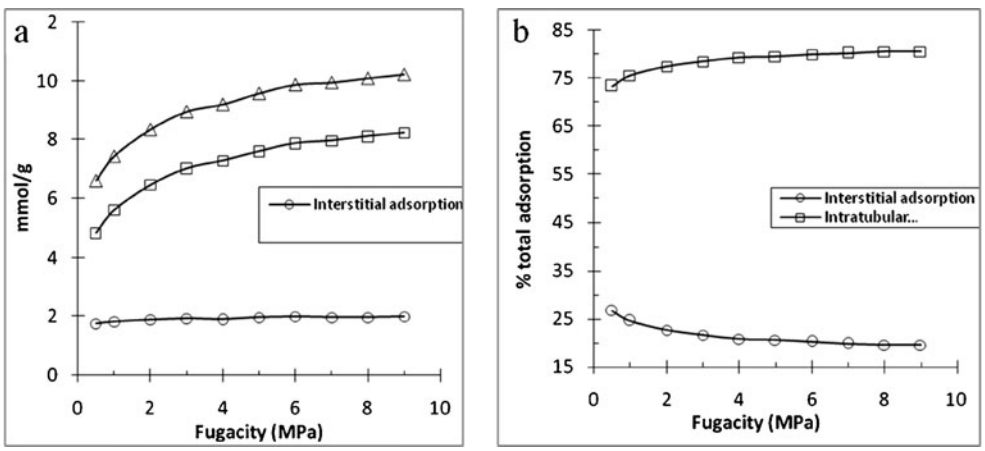

Fig. 12 Interstitial, intertubular, and total adsorption isotherms of methane in a (14,14) SWBNNT array at T=298 K (**a**); contributions of interstitial and intertubular adsorption to the total adsorption (**b**)

Table 2 The calculated isotherm parameters

Isotherm models	(8,8)		(10,10)		(12,12)		(14,14)	
	Parameters	R^2	Parameters	R^2	Parameters	R^2	Parameters	R^2
Langmuir (T=298)	K=271200 q_m=4.286	0.928	K=309500 q_m=5.769	0.963	K=564300 q_m=9.452	0.977	K=717900 q_m=11.01	0.986
Langmuir (T=373)	K=556300 q_m=3.887	0.966	K=666400 q_m=5.237	0.991	K=1394000 q_m=8.347	0.995	K=1389000 q_m=9.568	0.991
Freunlich (T=298)	K=1.877 n=0.005	0.953	K=2.194 n=0.006	0.978	K=1.898 n=0.01	0.984	K=1.299 n=0.129	0.990
Freunlich (T=373)	K=0.837 n=0.009	0.996	K=0.742 n=0.118	0.991	K=0.237 n=0.214	0.991	K=0.281 n=0.212	0.995
Sips (T=298)	K=17540 q_m=5.288 n=4.564	0.954	K=40910 q_m=6.785 n=3.503	0.981	K=282700 q_m=10.86 n=2.282	0.990	K=567800 q_m=12.94 n=2.082	0.995
Sips (T=373)	K=46290 q_m=6.906 n=5.374	0.996	K=45350 q_m=5.838 n=1.828	0.998	K=164100 q_m=9.633 n=1.534	0.999	K=2.364000 q_m=12.45 n=1.912	0.999

for CH_4 storage (180 v/v at 298 K and 35 bar) using the SWBNNT array with nanotube diameters of 16.62 and 19.41 Å, respectively, as adsorbent. Our results indicate that SWBNNTs have greater methane storage capacity than their corresponding SWCNTs, and are a promising material that can be utilized for adsorbed natural gas processes.

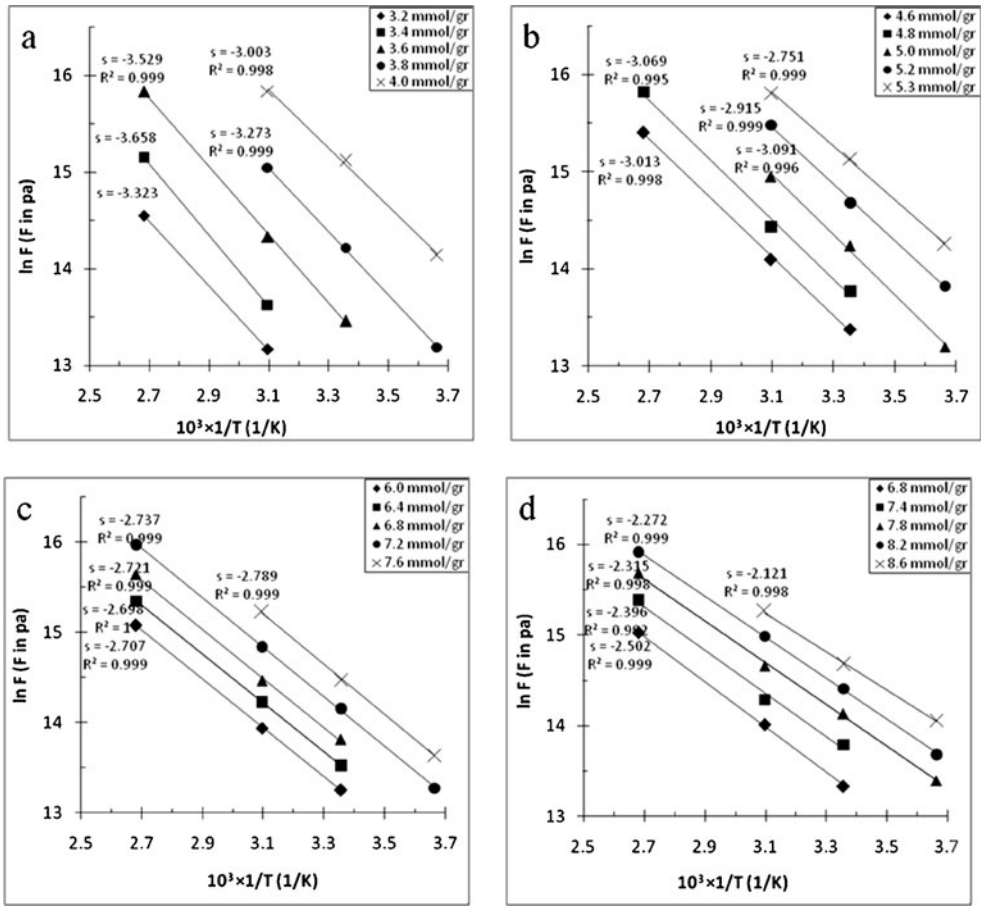

Fig. 13 The logarithmic form of the equilibrium pressure plotted against the reciprocal temperature at constant coverage for nanotube arrays with D=11.08 Å (**a**), D=13.85 Å (**b**), D=16.62 Å (**c**), and D=19.41 Å (**d**). s slope

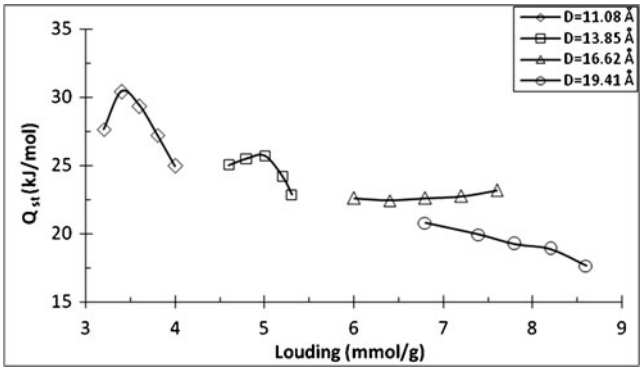

Fig. 14 Q_{st} as a function of CH_4 loading for different nanotube diameters

Table 3 Calculated specific surface area (m^2/g)

Specific surface area	(8,8)	(10,10)	(12,12)	(14,14)
BET surface	203	303	437	564
Langmuir surface	1134	1120	1185	1091

Appendix

Table 4 Different isotherm models

Isotherm	Equation	Parameters
Langmuir	$P = K\frac{q}{q_m - q}$	K,q_m
Freunlich	$P = \left(\frac{q}{K}\right)^{\frac{1}{n}}$	K, n
Sips	$P = K\left[\frac{q}{q_m - q}\right]^n$	K, q_m, n

References

1. Ishii T, Sato T, Sekikawa Y, Iwata M (1981) Growth of whiskers of hexagonal boron nitride. J Cryst Growth 52:285–289
2. Rubio A, Corkill JL, Cohen M (1994) Theory of graphitic boron nitride nanotubes. Phys Rev B 49:5081–5084
3. Blasé X, Rubio A, Louie SG, Cohen M (1994) Stability and band gap constancy of boron nitride nanotubes. Europhys Lett 28:335–340
4. Chopra NG, Luyken RJ, Cherrey K, Crespi VH, Cohen ML, Louie SG et al (1995) Boron nitride nanotubes. Science 269:966–967
5. Golberg D, Bando Y, Eremets M, Takemura K, Kurashima K, Yusa H (1996) Nanotubes in boron nitride laser heated at high pressure. Appl Phys Lett 69:2045–2047
6. Lourie OR, Jones CR, Bartlett BM, Gibbons PC, Ruoff RS, Buhro WE (2000) CVD growth of boron nitride nanotubes. Chem Mater 12:1808–1810
7. Chen Y, Gerald JF, Williams JS, Willis P (1999) Mechanochemical synthesis of boron nitride nanotubes. Mater Sci Forum 312:173–178
8. Han WQ, Bando Y, Kurashima K, Sato T (1998) Synthesis of boron nitride nanotubes from carbon nanotubes by a substitution reaction. Appl Phys Lett 73:3085–3087
9. Zhao JX, Ding YH (2008) Theoretical studies of the interaction of an open-ended boron nitride nanotube (BNNT) with gas molecules. J Phys Chem C 112:20206–20211
10. Mpourmpakis G, Froudakis GE (2007) Why boron nitride nanotubes are preferable to carbon nanotubes for hydrogen storage? An ab initio theoretical study. Catal Today 120:341–345
11. Cheng J, Zhang L, Ding R, Ding Z, Wang X, Wan Z (2007) Grand canonical Monte Carlo simulation of hydrogen physisorption in single-walled boron nitride nanotubes. Int J Hydrogen Energy 32:3402–3405
12. Han SS, Kang JK, Lee HM (2005) Theoretical study on interaction of hydrogen with single-walled boron nitride nanotubes. II. Collision, storage, and adsorption. J Chem Phys 123:114704
13. Chen X, Gao XP, Zhang H, Zhou Z, Hu WK, Pan GL et al (2005) Preparation and electrochemical hydrogen storage of boron nitride nanotubes. J Phys Chem B 109:11525–11529
14. Lim SH, Luo J, Ji W, Lin J (2007) Synthesis of boron nitride nanotubes and its hydrogen uptake. Catal Today 120:346–350
15. Oku T, Kuno M, Narita I (2004) Hydrogen storage in boron nitride nanomaterials studied by TG/DTA and cluster calculation. J Phys Chem Solids 65:549–552
16. Han SS, Lee SH, Kang JK, Lee HM (2005) High coverage of hydrogen on a (10,0) single-walled boron nitride nanotube. Phys Rev B 72:113402
17. Oku T, Narita I (2002) Calculation of H_2 gas storage for boron nitride and carbon nanotubes studied from the cluster calculation. Phys B 323:216–218
18. Jhi SH, Kwon YK (2004) Hydrogen adsorption on boron nitride nanotubes: a path to room-temperature hydrogen storage. Phys Rev B 69:245407
19. Ma R, Bando Y, Zhu H, Sato T, Xu C, Wu D (2002) Hydrogen uptake in boron nitride nanotubes at room temperature. J Am Chem Soc 124:7672–7673
20. Cheng J, Ding R, Liu Y, Ding Z, Zhang L (2007) Computer simulation of hydrogen physisorption in single-walled boron nitride nanotube arrays. Comput Mater Sci 40:341–344
21. Margulis VA, Muryumin EE, Tomilin OB (2006) Atomic hydrogen adsorption on boron nitride nanotube surfaces. Hydrogen Mater Sci Chem Carbon Nanomater 3:275–278
22. Chen Y, Hu CL, Li JQ, Jia GX, Zhang YF (2007) Theoretical study of O_2 adsorption and reactivity on single-walled boron nitride nanotubes. Chem Phys Lett 449:149–154
23. Beheshtian J, Behzadi H, Esrafili MD, Shirvani BB, Hadipour NL (2010) A computational study of water adsorption on boron nitride nanotube. Struct Chem 21:903–908
24. Zheng JW, Zhang LP, Wu P (2010) Theoretical study of Li, Si, and Sn adsorption on single-walled boron nitride nanotubes. J Phys Chem C 114:5792–5797
25. Li J, Zhou G, Liu H, Duan W (2006) Selective adsorption of first-row atoms on BN nanotubes. Chem Phys Lett 426:148–154
26. Zhao JX, Ding YH (2008) Theoretical study of Ni adsorption on single-walled boron nitride nanotubes with intrinsic defects. J Phys Chem C 112(5778):5783
27. Wu X, Zeng XC (2006) Adsorption of transition-metal atoms on boron nitride nanotube: a density-functional study. J Chem Phys 125:044711
28. Mukhopadhyay S, Gowtham S, Scheicher RH, Pandey R, Karna SP (2010) Theoretical study of physisorption of nucleobases on boron nitride nanotubes: a new class of hybrid nano-biomaterials. Nanotechnology 21:165703
29. Makogon YF (2010) Natural gas hydrates—a promising source of energy. J Nat Gas Sci Eng 2:49–59

30. Sabo K, Scitovski R, Vazler I, Zekić-Sušac M (2011) Mathematical models of natural gas consumption. Energy Convers Manage 52:1721–1727
31. Di Pascoli S, Femia A, Luzzati T (2001) Natural gas, cars and the environment. A clean and cheap fuel. Ecol Econ 38:179–189
32. Ruester S, Neumann A (2008) The prospects for liquefied natural gas development in the US. Energy Policy 36:3160–3168
33. Gupta A, Chempath S, Sanborn MJ, Clark LA, Snurr RQ (2003) Object-oriented programming paradigms for molecular modeling. Mol Simul 29:29–46
34. Allen MP, Tildesley DJ (1987) Computer simulation of liquids. Clarendon, Oxford
35. Martin MG, Siepmann GI (1998) Transferable potentials for phase equilibria 1. United-atom description of *n*-alkanes. J Phys Chem B 102:2569–2577
36. Liu Z, Marder TB (2008) B–N versus C–C: how similar are they? Angew Chem Int Ed 47:242–244
37. Wang Y, Yamamoto Y, Kiyono H, Shimada S (2008) Highly ordered boron nitride nanotube arrays with controllable texture from ammonia borane by template-aided vapor-phase pyrolysis. J Nanomater 2008:606283
38. Marom N, Bernstein J, Garel J, Tkatchenko A, Joselevich E, Kronik L et al (2010) Stacking and registry effects in layered materials: the case of hexagonal boron nitride. Phys Rev Lett 105:046801
39. Vlugt TJH, Schenk M (2002) Influence of framework flexibility on the adsorption properties of hydrocarbons in the zeolite silicalite. J Phys Chem B 106:12757–12763
40. Frenkel D, Smit B (2002) Understanding molecular simulations, from algorithms to applications, 2nd edn. Academic, San Diego
41. Jakobtorweihen S, Hansen N, Keil FJ (2006) Combining reactive and configurational-bias Monte Carlo: Confinement influence on the propene metathesis reaction system in various zeolites. J Chem Phys 125:224709
42. Poling BE, Prausnitz JM, O'Connell J (2000) The properties of gases and liquids, 5th edn. McGraw-Hill, New York
43. Mahdizadeh SJ, Tayyari SF (2011) Influence of temperature, pressure, nanotube's diameter and intertube distance on methane adsorption in homogeneous armchair open-ended SWCNT triangular arrays. Theor Chem Acc 128:231–240
44. Biloe S, Goetz V (2001) Dynamic discharge and performance of a new adsorbent for natural gas storage. AICHE J 47:2819–2830
45. Talapatra S, Migone AD (2002) Adsorption of methane on bundles of closed-ended single-wall carbon nanotubes. Phys Rev B 65:045416
46. Peralta-Inga Z, Lane P, Murray JS, Boyd S, Grice ME, O'Connor CJ et al (2003) Characterization of surface electrostatic potentials of some (5,5) and (n,1) carbon and boron/nitrogen model nanotubes. Nano Lett 3:21–28
47. Janik JF, Ackerman WC, Paine RT, Hua DW, Maskara A, Smith DM (1994) Boron nitride as a selective gas adsorbent. Langmuir 10:514–518